SPARSE ATTENTION WITH LEARNING-TO-HASH

Anonymous authors
Paper under double-blind review

ABSTRACT

Transformer has become ubiquitous in sequence modeling tasks. As a key component of Transformer, self-attention does not scale to long sequences due to its quadratic time and space complexity with respect to the sequence length. To tackle this problem, recent work developed dynamic attention sparsification techniques based on Approximate Nearest Neighbor (ANN) methods, where similar queries and keys are allocated to the same hash bucket with high probability. However, the effectiveness of those ANN methods relies on the assumption that queries and keys should lie in the same space, which is not well justified. Besides, some of the ANN methods such as Locality-Sensitive Hashing (LSH) are randomized and cannot fully utilize the available real data distributions. To overcome these issues, this paper proposes a new strategy for sparse attention, namely LHA (Learning-to-Hash Attention), which directly learns separate parameterized hash functions for queries and keys, respectively. Another advantage of LHA is that it can be used as a plug-and-play replacement for dense attention layers without imposing extra constraints for queries and keys, which makes it applicable to the wide range of pre-trained Transformer models. Our experiments on evaluation of the WikiText-103 dataset for language modeling, the GLUE benchmark for natural language understanding, and the Lang-Range-Arena benchmark for multiple tasks (text/image classification, retrieval, etc.) show the superior performance of LHA over other strong Transformer variants.

1 INTRODUCTION

The Transformer architecture (Vaswani et al., 2017) has been successfully applied to various tasks, including natural language processing (Vaswani et al., 2017; Devlin et al., 2018; Dai et al., 2019; Liu et al., 2019; Yang et al., 2019), computer vision (Carion et al., 2020; Dosovitskiy et al., 2020), and time series forecasting (Zhou et al., 2020; Wu et al., 2021). Such a success is mainly due to the self-attention component, which enables each token to directly interact with any other tokens in the entire sequence. But self-attention has a quadratic time and space complexity with respect to the sequence length and hence does not scale efficiently to long sequences as a result.

To address this inefficiency problem, one of the solutions is to approximate the full attention matrix with a sparse one, as the $\mathrm{softmax}$ operation is dominated by the largest elements. Some recent efforts focus on dynamic learning of sparse attention patterns via Approximate Nearest Neighbors (ANN) approaches, including Locality Sensitive Hashing (LSH) (Kitaev et al., 2020; Daras et al., 2020) and mini-batch spherical k-means (Roy et al., 2021; Wang et al., 2020a). The queries and keys are hashed or clustered into different buckets, hoping that the queries and keys in the same bucket are similar with a high probability. The effectiveness of those ANN approaches rely on the assumption that the (transformed) query and key vectors should lie in the same space, which could be sub-optimal in dealing with different sparsity patterns, as analyzed in this paper (Section 3.2). Besides, the hash functions in LSH are randomized and data-agnostic, which cannot fully utilize the rich information in real-world data distributions.

In this paper, we address the above limitations of existing ANN-based methods for attention sparsification. Firstly, we analyze two imbalance issues in LSH-produced sparse attention patterns, i.e., unbalanced hash bucket sizes and unbalanced query-key ratios. Secondly, we design a new metric called attention utility to quantify how well the sparse patterns approximate the full attention, and we show that ANN-derived sparse patterns are substantially inferior to their counterparts. Thirdly, we propose a novel solution, namely Learning-to-Hash Attention (LHA), for dynamic attention

sparsification with enhanced model expressiveness. LHA directly optimizes our newly defined attention utility metric in an end-to-end manner via separate learnable hash functions for queries and keys, respectively. As for reducing the computational complexity in the training phase, LHA uses unbiased kernelized attention techniques (Choromanski et al., 2020; Peng et al., 2021) to efficiently approximate the attention utilities. Similar to other sparse attention models (Kitaev et al., 2020; Roy et al., 2021), LHA reduces the overall complexity of self-attention from $\mathcal{O}(N^2)$ to $\mathcal{O}(N^{1.5})$ for sequence length N. Our experiments in a wide range of tasks on the evaluation benchmarks for language modeling, natural language understanding, and Long-Range-Arena show that LHA achieves better performance compared to strong transformer baselines.

2 Related Work

Related work can be roughly divided into three categories, i.e., location-based sparse attention, content-based sparse attention, and dense approximation of attention, as outlined below.

Location-based sparse attention methods aim to improve the computational efficiency by using pre-specified global or local sparsification patterns over token locations. Liu et al. (2018) proposed to alternate coarse attention layers and local attention layers. Child et al. (2019) used a strided sparse attention pattern in image generation. Sukhbaatar et al. (2019) imposed sparsity based on the predicted temporal window size for each token. Other methods (Zhang et al., 2021; Beltagy et al., 2020; Ainslie et al., 2020; Zaheer et al., 2020) used a pre-specified subset of locations in the input as the global memory, and only allow non-local attentions from this subset to all the other tokens. Location-based sparse attention cannot leverage more flexible content-based interactions among arbitrary positions, as a limitation.

Content-based sparse attention allows more flexible sparse attention patterns than location-based ones. Malaviya et al. (2018) used $\mathrm{sparsemax}$ to obtain a sparse attention matrix, while (Correia et al., 2019) used entmax instead of $\mathrm{softmax}$. These methods require to compute the full attention matrix before sparsification and hence cannot reduce the quadratic computation complexity. Approximate Nearest Neighbor (ANN) methods address this limitation by calculating the content-based sparse patterns in advance (Roy et al., 2021; Kitaev et al., 2020; Daras et al., 2020; Wang et al., 2020a) (which will be discussed more in Section 3.1). Those methods usually apply an ANN module as the shared hash function to both queries and keys. Vyas et al. (2020) and Zhou et al. (2020) sparsified the attention maps by eliminating redundant queries. Tay et al. (2020b) designed a differentiable sorting algorithm of internal representations to enable efficient quasi-global local attention.

Another line of research explored low-rank or kernelized dense approximation of attention matrices, instead of computing the attention scores exactly for only a few pairs. Wang et al. (2020b) applied a low-rank decomposition to the attention matrix. Xiong et al. (2021) approximated the attention matrix with Nyström approximation. Katharopoulos et al. (2020) utilized the association property of Key-Query-Value multiplication and reduce the quadratic complexity to linear complexity with kernelized approximation to the $\mathrm{softmax}$ operation. Choromanski et al. (2020) and Peng et al. (2021) further proposed an unbiased approximation of $\mathrm{softmax}$ with random Fourier features.

Our work in this paper is directly related to the second category, i.e., content-based attention sparsification. Specially, we address the limitations of existing ANN-based methods by modeling queries and keys in separate vector spaces and by proposing a novel approach to learn the hash functions for attention sparsification.

3 Re-examination of Content-based Sparse Patterns

3.1 Preliminary

The self-attention mechanism (Vaswani et al., 2017) can be formulated as the weighted sum of the value vectors $V \in \mathbb{R}^{N \times d_h}$ where the weights are calculated using query vectors $Q \in \mathbb{R}^{N \times d_h}$ and key vectors $K \in \mathbb{R}^{N \times d_h}$ as:

$$\text{Attention}(Q, K, V) = A \cdot V = \mathrm{softmax}\left(\frac{QK^T}{\sqrt{d_h}}\right) \cdot V, \tag{1}$$

where A denotes the matrix of normalized attention weights, d_h is the dimension of hidden representations, and N is the sequence length. self-attention has a quadratic time and space complexity with respect to the sequence length and hence does not scale efficiently to long sequences.

Content-based sparse attention methods usually apply randomized hash functions or a clustering algorithm to queries $\{Q_i\}$ and keys $\{K_j\}$, and hope that similar queries and keys are hashed or clustered into the same bucket. The queries can thus only attend to the keys if both are in the same bucket. Formally, a content-based sparse attention strategy with B hash buckets is defined as:

$$\text{Sparse-Attention}(Q_i, K, V) = \sum_{j:h_Q(Q_i)=h_K(K_j)} \bar{A}_{ij} V_j, \tag{2}$$

where $h_K, h_Q : \mathbb{R}^{d_h} \mapsto [B]$ are the hash functions for keys and queries, and $\bar{A}_{ij} \propto A_{ij}$ is the re-normalized attention weights such that $\forall i,\ \sum_{j:h_Q(Q_i)=h_K(K_j)} \bar{A}_{ij} = 1$. In general (Kitaev et al., 2020; Roy et al., 2021), calculating the hash function and performing local attention for each query have the time complexity of $\mathcal{O}(B)$ and $O(N/B)$, respectively. Thus, the overall complexity[1] of self-attention can be reduced from $\mathcal{O}(N^2)$ to $\mathcal{O}(N \cdot B + N^2/B) \approx \mathcal{O}(N^{1.5})$ when $B \approx N/B \approx \sqrt{N}$.

Since the hash functions are not differentiable, Approximate Nearest Neighbor (ANN) methods are used to derive an effective content-based hash function. Reformer (Kitaev et al., 2020) applies Locality Sensitive Hashing (LSH) to the tied queries and keys, where several hyper-planes are randomly generated to divide tokens into different buckets. SMYRF (Daras et al., 2020) improves Reformer by introducing asymmetric transformation to queries and keys, i.e.,

$$F(Q_i) = \left[Q_i; 0; \sqrt{M_Q^2 + M_K^2 - ||Q_i||_2^2}\right], \quad G(K_j) = \left[K_j; \sqrt{M_Q^2 + M_K^2 - ||K_j||_2^2}; 0\right], \tag{3}$$

where $M_Q = \max_{Q_i} ||Q_i||_2$ and $M_K = \max_{K_j} ||K_j||_2$, such that $||F(Q_i) - G(K_j)||_2^2 = const - Q_i \cdot K_j$. Routing Transformer (Roy et al., 2021) and Cluster-former (Wang et al., 2020a) use mini-batch spherical k-means to partition tokens into different clusters.

3.2 Bucket Imbalance Issues

Previous content-based sparse attention models take it for granted that the ANN-derived sparse pattern can effectively approximate the full attention. However, it is only verified via empirical evaluation on the down-stream tasks yet, which cannot reflect the true attention map approximation ability. Notice that there are two necessary conditions for sparse attention to work effectively and efficiently:

1. The number of queries and the number of keys in each bucket should be reasonably balanced, as queries should attend to enough keys to get a good approximation of the full-attention;
2. The bucket sizes should be nearly equal in order to effectively reduce the overall complexity.

We first analyze how badly the two conditions would be violated by LSH[2], a typical ANN method. We apply LSH to 10 attention heads in the 3rd layer of a Transformer pre-trained on language modeling and obtain the results shown in Figure 1 (up). We can see that the imbalance issue not only exists in the query-key ratios, but also in the bucket sizes. To go a step further, we apply LSH to all $16 \times 10 = 160$ attention heads in the pre-trained Transformer and find that around **61.3%** buckets have the query-key imbalance problem, where the query-key ratios are either greater than 2:1 or smaller than 1:2. Around **35.9%** buckets have the bucket size imbalance problem, where the bucket sizes are twice greater than half smaller than the expected bucket size of 512. Clearly, neither of the two aforementioned conditions are well satisfied in this LSH-sparsified Transformer model.

There can be several possible reasons that cause the imbalance problem: 1) the Euclidean distance metric in ANN methods does not monotonically decrease with the dot-product metric used in attention mechanism; 2) the queries and keys are from different distribution and not normalized, and thus restricts the effectiveness of ANN methods. To investigate the root cause, we apply the SMYRF

[1] Notice that we only consider the setting of single-round hashing in our paper, but our analysis and the proposed LHA method can be generalized to the multi-round hashing setting.

[2] We use the same LSH technique as in (Kitaev et al., 2020), except that we do not impose extra constraints to queries and keys. The detailed experimental setting can be found in the appendix.

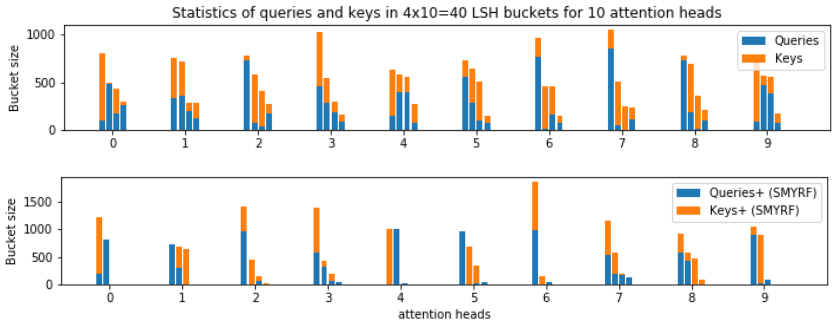

Figure 1: We show the unbalanced bucket sizes and unbalanced query-key ratios with statistics of 10 attention heads in the 3rd layer of a pre-trained Transformer. For each head, we assign the queries and keys of first 1024 tokens in the WikiText-103 validation data into 4 LSH buckets. The buckets are sorted for each attention head according to total bucket sizes (i.e., #query + #key).

asymmetric transformation (Equation 3) to queries and keys, which creates a monotonic relation between Euclidean distances and dot-products. The new analysis results are shown in Figure 1 (down). We can see that the asymmetric transformation would only exacerbate the imbalance problem, with respect to both query-key ratios and bucket sizes. Therefore, we can conclude that the root cause of the imbalance problem is the mismatch between the query and key distributions, that could be further magnified by the asymmetric transformation.

3.3 Proposed Metric: Attention Utility

The above analysis shows the imbalance problem in ANN-derived hashing strategies. To further quantify the approximation quality of sparse attention patterns, we utilize the concept of Attention Biclustering from (Daras et al., 2020), which considers a practical case (Kitaev et al., 2020; Roy et al., 2021) where all clusters strictly contain the same number of queries and keys:

$$\forall b \in [B], \quad |\{Q_i \mid h_Q(Q_i) = b\}| = |\{K_j \mid h_K(K_j) = b\}| = \frac{N}{B}. \tag{4}$$

We denote with $\mathcal{C}$ the set of all possible assignments in B balanced non-overlapping clusters: $\mathcal{C} = \{\mathcal{C}_1, \mathcal{C}_2, \ldots, \mathcal{C}_T\}$, where T is the number of possible assignments. We can then define the attention utility AU of each assignment C_t as:

$$\mathrm{AU}(\mathcal{C}_t) = \sum_{i,j:(Q_i,K_j)\in\mathcal{C}_t} A_{ij}, \quad \text{where} \quad \mathcal{C}_t = \{(Q_i, K_j) | h_Q^{\mathcal{C}_t}(Q_i) = h_K^{\mathcal{C}_t}(K_j)\}. \tag{5}$$

The attention utility represents the aggregation of the sparse attention weights in an assignment. As we should keep as much sparse attention weights as possible to better approximate a full attention map, attention utility quantifies how well a sparse attention approximates the full one. In fact, we can show that it is computationally intractable to find the optimal attention utility:

Theorem 1. *Finding the assignment that achieves the optimal attention utility, i.e.,*

$$\arg\max_{\mathcal{C}_t \in \mathcal{C}} \mathrm{AU}(\mathcal{C}_t) = \sum_{(Q_i,K_j)\in\mathcal{C}_t} A_{ij} \tag{6}$$

is NP-hard.

This theorem is a corollary of the NP-hardness of Attention Biclustering in (Daras et al., 2020), and it motivates us to develop a learning-based approach to optimize the attention utility. Notice that similar to other sparse attention models (Kitaev et al., 2020; Roy et al., 2021), the proposed attention utility metric currently does not take causal masks into consideration. Developing a new metric that can take arbitrary attention masks into account is left for future work.

To measure the attention utility of ANN-derived sparse attention patterns, we follow (Kitaev et al., 2020; Daras et al., 2020) and adaptively set hash boundaries to create balanced clusters. The analyzed models include LSH, LSH with asymmetric transformation (i.e., SMYRF), and our proposed Learning-to-Hash (L2H) method which will be introduced in the next section. We also calculate the empirical

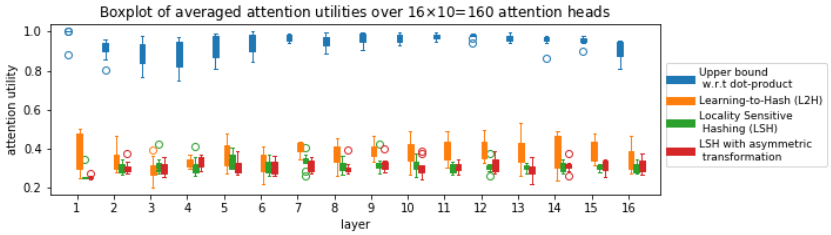

Figure 2: We show the attention utility evaluation of four different sparse attention patterns. For L2H and LSHs, we assign the queries and keys of first 1024 tokens in the WikiText-103 validation data into 4 hash buckets. The causal mask is not used when calculating the attention weights.

upper bound by aggregating the attention from each query to its top keys w.r.t dot-products. We present a box-plot of averaged attention utilities for all 16 Transformer layer in Figure 2. We can see that the LSH methods obtain significantly less attention utilities than the upper bound or L2H. As a conclusion, the ANN-derived sparse patterns are arguably sub-optimal when used as hash functions for sparse attention. We believe this also partially explains why most of these approaches need to impose extra constraints (e.g. queries and keys are tied or normalized). In the next section, we propose an alternative choice of the hash functions to tackle this problem.

4 Learning-to-Hash Attention (LHA)

We propose a novel Learning-to-Hash Attention model in this section. The key idea is to learn separate parameterized hash functions for queries and keys, respectively, thus the sparse pattern in LHA can be no longer limited to distance-based hash functions such as LSH or online k-means and adapt to the mismatch of query and key distributions. Besides, we empirically find that LHA can be used as a plug-and-play replacement for dense attention layers, which makes LHA applicable to the wide range of pre-trained Transformer models.

4.1 Learning-to-Hash for Sparse Attention

We first remind the readers of our definitions of the sparse attention:

$$\text{Sparse-Attention}(Q_i, K, V) = \sum_{j:h_Q(Q_i)=h_K(K_j)} \bar{A}_{ij} V_j \tag{7}$$

where $h_K, h_Q : \mathbb{R}^{d_h} \mapsto [B]$ are the hash functions for keys and queries, and $\bar{A}_{ij} \propto A_{ij}$ is the re-normalized attention weights such that $\forall i, \sum_{j:h_Q(Q_i)=h_K(K_j)} \bar{A}_{ij} = 1$. Inspired by the Learning-to-Hash methods (Wang et al., 2017), we implement the learnable hash functions $h_K, h_Q : \mathbb{R}^{d_h} \mapsto [B]$ by defining parameterized functions $H_Q, H_K : \mathbb{R}^{d_h} \mapsto \mathbb{R}^B$, such that:

$$h_Q(Q_i) = \underset{b\in\{1,\ldots,B\}}{\arg\max} \left[H_Q(Q_i)\right]_b, \quad h_K(K_j) = \underset{b\in\{1,\ldots,B\}}{\arg\max} \left[H_K(K_j)\right]_b, \tag{8}$$

where H_Q and H_K can be any parameterized functions such as MLPs.

Notice that our formulation is a generalization of the non-learnable sparse attention mechanisms in several previous content-based sparse attention models. To reproduce the symmetric LSH-based sparse attention scheme in Reformer (Kitaev et al., 2020) or the mini-batch k-means scheme in Routing Transformer (Roy et al., 2021), we can set:

$$H_Q(x) = H_K(x) = x[\mathbf{R}; -\mathbf{R}] \quad \text{or} \quad H_Q(x) = H_K(x) = x\boldsymbol{\mu} \tag{9}$$

where $\mathbf{R} \in \mathbb{R}^{d_h \times \frac{B}{2}}$ is a random matrix, $[\cdot;\cdot]$ denotes the concatenation of two vectors, and $\boldsymbol{\mu} \in \mathbb{R}^{d_h \times B}$ are the exponentially moving averaged cluster centroids shared by keys and queries. The asymmetric transformation in SMYRF (Daras et al., 2020) can also be reproduced by:

$$H_Q(x) = \mathbb{1}\left(\left\lfloor \frac{F(x)\cdot \mathbf{a} + \mathrm{b}}{r} \right\rfloor\right), \qquad H_K(x) = \mathbb{1}\left(\left\lfloor \frac{G(x)\cdot \mathbf{a} + \mathrm{b}}{r} \right\rfloor\right) \tag{10}$$

where $\mathbf{a}$ is a random vector, b is a random scalar, r is a scalar parameter, $\mathbb{1}(\cdot) : [B] \mapsto \{0,1\}^B$ is the one-hot operation, and $F(\cdot)$ and $G(\cdot)$ are defined as in Equation 3.

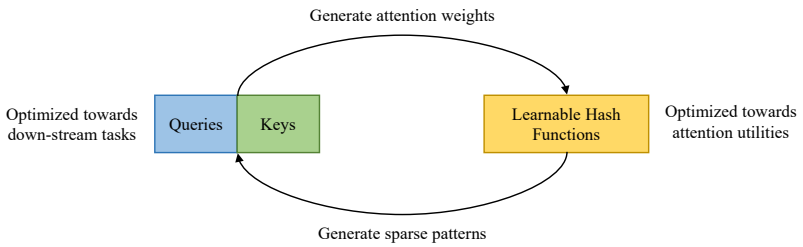

Figure 3: The joint training diagram of LHA, where queries and keys generate attention weights to train the learnable hash functions, while the hash functions generate the sparse attention patterns, on which queries and keys are trained towards down-stream tasks.

4.2 Optimization Objective for Learning-to-Hash

Previous ANN-derived sparse attention models construct their hash functions by either randomization or k-mean clustering. In contrast, our hash functions are fully learnable. However, as we use the $\arg\max$ operation to get the hashing buckets, the parameterized projections in our hash functions cannot be trained in an end-to-end manner. To resolve this issue, we guide the training of our learnable hash functions directly by our proposed attention utility (See Equation 5). Notice that the attention utility of each query Q_i can be written as $\sum_{j:h_Q(Q_i)=h_K(K_j)} A_{ij}$. We first calculate the possible attention utilities $\boldsymbol{\psi}^{(i)}$ that query Q_i can obtain when allocated to all B hash buckets:

$$\boldsymbol{\psi}^{(i)} = \left(\sum_{j:h_K(K_j)=0} A_{ij}, \cdots, \sum_{j:h_K(K_j)=B-1} A_{ij} \right) \tag{11}$$

Ideally, our hash function would allocate Q_i to the bucket that maximize the attention utility, such that Q_i can attend to the most salient keys:

$$h_Q(Q_i) = \arg\max_{b\in[N_b]} \boldsymbol{\psi}_b^{(i)} = \arg\max_{b\in[B]} \sum_{h_K(K_j)=b} A_{ij} \tag{12}$$

To achieve this goal, since $\boldsymbol{\psi}^{(i)}$ is naturally a normalized categorical distribution, we can simply convert $H_Q(Q_i)$ into a distribution and use the KL divergence between the predicted distribution $\mathrm{softmax}(H_Q(Q_i))$ and the desired distribution $\boldsymbol{\psi}^{(i)}$ as the optimization objective:

$$\mathcal{L}_{Q_i} = KL(\boldsymbol{\psi}^{(i)} \| \mathrm{softmax}(H_Q(Q_i))) \tag{13}$$

On the other hand, the possible attention utilities $\boldsymbol{\psi}'^{(j)}$ that a key Q_i obtains when allocated to all B buckets can be written as:

$$\boldsymbol{\psi}'^{(j)} = \left(\sum_{i:h_Q(Q_i)=0} A_{ij}, \cdots, \sum_{i:h_Q(Q_j)=B-1} A_{ij} \right) \tag{14}$$

While $\boldsymbol{\psi}'^{(j)}$ is not longer a normalized distribution, we can normalize it and similarly define the optimization objective $\mathcal{L}_{K_j}$ also as a KL divergence.

During the training stage, our final optimization objective is a convex combination of the task-specific objective and the learning-to-hash objectives (i.e., $\{\mathcal{L}_{Q_i}\}$ and $\{\mathcal{L}_{K_j}\}$) for all queries and keys. Figure 3 illustrates the joint training diagram of LHA.

4.3 Approximate Attention Utilities

The remaining problem is how to efficiently compute $\boldsymbol{\psi}^{(i)}$ and $\boldsymbol{\psi}'^{(j)}$. A naive way requires calculating the dot products between all query-key pairs with $\mathcal{O}(N^2)$ complexity. Inspired by the recent advances in kernelized attention (Katharopoulos et al., 2020; Choromanski et al., 2020; Peng et al., 2021), we use random Fourier features (Rahimi et al., 2007; Choromanski et al., 2020) to approximate $\boldsymbol{\psi}^{(i)}$ in an unbiased manner. Let us define $\boldsymbol{\phi} : \mathbb{R}^{d_h} \mapsto \mathbb{R}^{2D}$ as the Positive Randomized Features (PRFs) (Choromanski et al., 2020) such that

$$\mathbb{E}[\boldsymbol{\phi}(\mathbf{x}) \cdot \boldsymbol{\phi}(\mathbf{y})] = \exp\left(\frac{\mathbf{x}^T\mathbf{y}}{\sqrt{d_h}}\right) \tag{15}$$

We can approximate $\boldsymbol{\psi}^{(i)}$ with the following formula:

$$\boldsymbol{\psi}_b^{(i)} = \sum_{j:h_K(K_j)=b} A_{ij} \propto \sum_{j:h_K(K_j)=b} \exp\left(\frac{Q_i \cdot K_j}{\sqrt{d_h}}\right) \propto \mathbb{E}\left[\boldsymbol{\phi}(Q_i) \cdot \sum_{j:h_K(K_j)=b} \boldsymbol{\phi}(K_j)\right] \tag{16}$$

for each bucket $b \in [B]$. Since $h_K(K_j)$ does change for the queries, we can simply pre-compute $\sum_{j:h_K(K_j)=b} \boldsymbol{\phi}(K_j)$ once to save computation, which reduces the complexity of computing $\{\boldsymbol{\psi}^{(i)}\}$ for all queries from $\mathcal{O}(N^2)$ to $\mathcal{O}(N \cdot B) \approx \mathcal{O}(N^{1.5})$. The attention utilities for keys $\boldsymbol{\psi}'^{(j)}$ can be efficiently approximated in a similar way[3]:

$$\boldsymbol{\psi}_b'^{(i)} = \sum_{i:h_Q(Q_i)=b} A_{ij} \propto \mathbb{E}\left[\left(\sum_{j:h_Q(Q_i)=b} \frac{\boldsymbol{\phi}(Q_i)}{\boldsymbol{\phi}(Q_i) \cdot \sum_{j=1}^{N} \boldsymbol{\phi}(K_j)}\right) \cdot \boldsymbol{\phi}(K_j)\right] \tag{17}$$

4.4 Implementation Details

Practical content-based sparse attention models require that each hash bucket has the same size, which is crucial in terms of computational efficiency on modern hardwares.Therefore, we follow Roy et al. (2021) and sort the tokens with regard to normalized hash scores, i.e., softmax$(H_Q(Q_i))$ and softmax$(H_K(K_i))$, in each bucket. The hash bucket membership is then determined by the top-k threshold, where $k = \frac{N}{B}$ is the bucket size. Since such a bucketing strategy no longer guarantees the validation of attention bi-clustering, as each query or each key can be assigned to zero or more than one clusters, we further empirically enlarge the hash bucket sizes by $\sqrt{2}\times$ to increase the recall of queries and keys. A pseudo-code implementation for LHA can be found in the appendix.

In causally masked attentions, the queries cannot attend to keys behind, as is usually the case in language modeling. When we use separate hash functions $\{h_Q(Q_i)\}$ and $\{h_K(K_j\})$ for queries and keys, respectively, it is possible that for some query Q_i, there exists no such key K_j in the same bucket that $j \leq i$. This would cause serious numerical instability in our implementation. To tackle this problem, inspired by Kitaev et al. (2020) and Roy et al. (2021), we tie the key hashes with query hashes in the case of causal attentions by constructing a joint hash function:

$$h_K(K_i) = h_Q(Q_i) = \underset{b \in [N_b]}{\arg\max} \left[H_Q(Q_i)_b + H_K(K_i)_b\right] \tag{18}$$

We find that this strategy empirically works better than using other tricks to fix this "no-attention-target" problem. Our solution is different from Routing Transformer (Roy et al., 2021) or Reformer (Kitaev et al., 2020), which impose an extra constraint that queries and keys are tied.

5 Experiments

In this section, we conduct experiments to verify the effectiveness of our approach on several benchmark datasets covering language modeling, natural language understanding, and Long-Range-Arena. Due to the space limitations, the detailed hyper-parameter settings are presented in the appendix.

5.1 Language Modeling

`Wikitext-103` (Merity et al., 2016) is a large-scale dataset for testing long term dependencies in word-level language models. It contains 103M training tokens from 28K articles, with an average length of 3.6K tokens per article, which allows testing the ability of long-term dependency modeling. We use this dataset as a probe dataset to perform various ablations to tease apart the effect of various hyper-parameter choices on the model performance.

We follow the `base` setting of the state-of-the-art Transformer-XL (Dai et al., 2019) model, which contains 16 Transformer layers with 10 heads per layer. For local attentions, we use the relative positional encoding (Dai et al., 2019), while for non-local attentions (i.e., LSH or LHA), we use the

[3]Please refer to (Choromanski et al., 2020) for how PRFs stabilize attention renormalization.

Table 1: Ablation studies on the WikiText-103 validation data in the `base` setting. Lower perplexity (PPL) is better. All the models have a total of 16 attention layers and 10 heads. Non-Local (NL, i.e., LSH or LHA) layers when present are always added at the top of the model. Attention size denotes either local window size or hash bucket size. † denotes that the results are taken from Transformer-XL (Dai et al., 2019).

	label	NL Heads	NL Layers	Hash Func.	Att. Size	#Param	Valid PPL	Test PPL
Local Transformer	-	0	0	-	768	151M	22.89	-
	-	0	0	-	384	151M	23.82	-
	-	0	0	-	640	151M	23.09†	24.0†
LSH Transformer	-	10	16	Rand. Linear	384	153M	24.64	-
	-	5	0	Rand. Linear	384	153M	23.51	-
	-	0	8	Rand. Linear	384	153M	23.76	-
	-	5	8	Rand. Linear	384	153M	23.53	-
LHA Transformer	(a)	10	16	Rand.	384	153M	26.05	-
	(b)	10	16	Linear	384	153M	24.22	-
	(c)	10	16	MLP	384	153M	24.00	-
	(d)	5	0	MLP	384	153M	**22.79**	**23.2**
	(e)	0	8	MLP	384	153M	23.00	-
	(f)	5	8	MLP	384	153M	22.84	-

Table 2: Performance of methods per task on the GLUE benchmark, where C and $\#$ denote the number of queries/keys per cluster and hashing rounds, respectively. † denotes that the results are taken from their original papers.

	#	C	CoLA	MNLI	MRPC	QNLI	QQP	RTE	SST-2	STS-B	AVG
RoBERTa-base	-	-	60.9	87.6	88.7	92.7	**91.6**	68.5	94.5	**90.0**	84.3
SMYRF†	2	16	58.9	82.3	85.7	89.5	89.3	64.5	93.1	87.8	81.4
SMYRF†	2	32	58.8	85.0	87.7	91.1	89.7	68.6	93.2	89.7	83.0
FCA†	-	-	59.8	79.4	43.6	74.6	89.4	49.8	94.4	78.9	71.2
i-FCA†	-	-	60.1	88.0	87.3	**93.0**	91.5	**70.4**	94.7	**90.0**	84.4
LSH	1	11	61.5	86.3	88.7	91.1	90.2	68.0	93.3	88.5	83.5
LSH	1	22	61.5	86.8	**89.7**	91.9	90.8	68.4	93.9	88.7	84.0
LSH	1	45	61.8	87.5	88.7	92.7	91.2	68.1	94.0	89.4	84.2
LHA	1	11	61.2	85.7	89.1	91.3	90.5	68.0	93.7	89.0	83.6
LHA	1	22	62.0	86.8	88.0	92.4	91.1	68.6	**94.8**	89.6	84.2
LHA	1	45	**62.3**	**87.7**	89.1	92.8	91.4	68.5	94.6	89.5	**84.5**

per-layer sinusoidal absolute positional encoding (Vaswani et al., 2017). The LSH Transformer is implemented in our code base by simply replacing the learnable hash functions by random projections. A sequence length of 1536 is used in both training and evaluation stages for our models. In ablation study, we vary 1) the type of non-local attention heads, 2) the type of learnable hash function in LHA (i.e., linear or two-layer MLP), 3) the number of non-local attention heads, and 4) the number of non-local attention layers. We also consider a baseline where the hash functions generate content-independent random numbers. The experimental results are presented in Table 1.

From the table, we can see that a smaller attention size (384 compared to 768 in local Transformer) would decrease the model performance by 0.9, while adding LSH or LHA heads can improve the performance by 0.3 and 1.0, respectively. Surprisingly, we find that local Transformer is a very strong baseline for language modeling that outperforms a pure LHA Transformer. We can also see that a two-layer MLP works better than a linear function as the learnable hash functions in LHA. The best performance is achieved when we set half of the heads to local attention and the other half to non-local LHA for each layer. Finally, we can see that LHA consistently underperforms the untrainable LSH counterparts under four different settings. For the test set evaluation, we use the best setting from the ablation study. We can see that the proposed LHA model outperforms Transformer-XL, which further validate that LHA can help modeling long-term dependency for language modeling tasks.

5.2 Natural Language Understanding

To show the ability of our model to approximate arbitrarily complicated attention distributions, we evaluate our proposed method on the approximation of RoBERTa model (Liu et al., 2019) on the

Table 3: Accuracy on LO, IMDb, AAN, and Image in Long Range Arena benchmark. Best model per task is shown in boldface and second best is underlined. Throughput is evaluated on IMDb and relative to the vanilla transformer's. * and † denote that the best model is statistically significantly better ($p < 0.05$ in one-tail proportion test) than the vanilla Transformer baseline and the second best model, respectively. ‡ denotes that the throughput comparison are run on a single NVIDIA Tesla V100 32GB GPU, while previous results (Tay et al., 2020c) are reported on 4×4 TPU V3 chips.

	Accuracy (↑)					**Throughput** (↑)			
Model	**LO**	**IMDb**	**AAN**	**Image**	**Avg.**	**1K**	**2K**	**3K**	**4K**
Vaswani et al. (2017) - Transformer	36.4	64.3	57.5	42.4	<u>50.2</u>	1.0	1.0	1.0	1.0
Wang et al. (2020b) - Linformer	35.7	53.9	52.3	38.6	45.1	1.2	1.9	3.7	5.5
Kitaev et al. (2020) - Reformer	37.3	56.1	53.4	38.1	46.2	0.5	0.4	0.7	0.8
Child et al. (2019) - Sparse Trans.	17.1	63.6	<u>59.6</u>	<u>44.2</u>	46.1	-	-	-	-
Tay et al. (2020b) - Sinkhorn Trans.	33.7	61.2	53.8	41.2	47.5	1.1	1.6	2.9	3.8
Tay et al. (2020a) - Synthesizer	37.0	61.7	54.7	41.6	48.8	1.1	1.2	2.9	1.4
Zaheer et al. (2020) - BigBird	36.0	64.0	59.3	40.8	50.0	0.9	0.8	1.2	1.1
Katharopoulos et al. (2020) - Linear Trans.	16.1	65.9	53.1	42.3	44.4	1.1	**1.9**	3.7	5.6
Choromanski et al. (2020) - Performer	18.0	65.4	53.8	42.8	45.0	**1.2**	**1.9**	**3.8**	**5.7**
Peng et al. (2021) - RFA	<u>36.8</u>	<u>66.0</u>	56.1	-	-	1.1	1.7	3.4	5.3
Ours - LHA	**37.9**	**66.8***†	**62.8***†	**45.2***	**53.1**	1.0‡	1.1‡	1.3‡	1.5‡

GLUE (General Language Understanding Evaluation) dataset (Wang et al., 2018). Following the common practice, the maximum sequence length is set to 128. To show the effectiveness of LHA, we choose two competitive baselines in literature: SMYRF (Daras et al., 2020) and Fast Clustered Attention (FCA) (Vyas et al., 2020). We also produce an LSH-based sparse attention baseline. For a fair comparison, we use a pure LHA model similar to variant (c) in Section 5.1.

We summarize the performance per task in Table 2. We report accuracy for all tasks except STS-B, where we report Pearson correlation. From the table, we can see that LHA performs as good as full attention for all the GLUE tasks, and that LHA outperforms all other methods in the average GLUE score, and has a smaller computational costs in its sparse attention part.

5.3 Long-Range-Arena Benchmark

Long-Range-Arena (LRA) benchmark (Tay et al., 2020c) is a recently proposed benchmark focused on evaluating model quality under long-context scenarios for Transformer variants. We follow the apples-to-apples setting[4] of LRA benchmark and compare our method against other efficient attention variants. We use a LHA/local hybrid variant similar to variant (d) in Section 5.1.

We consider the tasks of ListOps (Nangia & Bowman, 2018) (LO), byte-level IMDb reviews text classification (Maas et al., 2011) (IMDb), byte-level document retrieval on ACL Anthology Network (AAN) (Radev et al., 2013), and CIFAR10 (Krizhevsky et al., 2009) image classification on sequences of pixels (Image). The results are shown in Table 3. We can see that LHA achieves consistent improvements over previous efficient attention models.

6 Conclusion & Future Work

In this paper, we address the limitations of ANN-based sparse attention methods and propose the Learning-to-Hash Attention (LHA) as our new solution. Specifically, LHA leverages separate learnable hash functions for queries and keys, respectively, and utilizes kernelized techniques for efficient approximation of attention utilities. The experiments on language modeling, natural language understanding, text classification, and image classification demonstrated the effectiveness of LHA. For future work, we would like to validate the effectiveness of LHA model on much larger language modeling datasets, such as `PG-19` (Rae et al., 2019).

[4] `www.github.com/google-research/long-range-arena#apples-to-apples-setting`

ETHICS STATEMENT

This work proposed a more effective sparsification pattern for the attention mechanisms. We believe our proposed model as well as the code to be released can most benefit the field of language processing, with the potential to benefit other fields involving long sequence modeling. However, it is know that Transformers are also vulnerable to the adversarial attacks (Michel et al., 2019). Since one of the advantage of our model is to re-use a pre-trained Transformer model, the effective adversarial perturbations on the pre-trained model could also be effective in our model.

REPRODUCIBILITY STATEMENT

- We will put a link to an anonymous repository for our source code as the OpenReview comment. The hyper-parameters are described in details in the appendix. We also provide a pseudo-code implementaion of our model in the appendix.
- All the datasets used in the experiments and the corresponding pre-processing scripts can be found online, including language modeling[5], GLUE benchmark[6], Long-Range-Arena benchmark[7], and time series forecasting[8]. The pre-trained model we used (i.e., RoBERTa) is also publically available[9].

REFERENCES

Joshua Ainslie, Santiago Ontanón, Chris Alberti, Vaclav Cvicek, Zachary Fisher, Philip Pham, Anirudh Ravula, Sumit Sanghai, Qifan Wang, and Li Yang. Etc: Encoding long and structured inputs in transformers. *arXiv preprint arXiv:2004.08483*, 2020.

Iz Beltagy, Matthew E Peters, and Arman Cohan. Longformer: The long-document transformer. *arXiv preprint arXiv:2004.05150*, 2020.

James Bradbury, Roy Frostig, Peter Hawkins, Matthew James Johnson, Chris Leary, Dougal Maclaurin, and Skye Wanderman-Milne. Jax: composable transformations of python+ numpy programs. *Version 0.1*, 55, 2018.

Nicolas Carion, Francisco Massa, Gabriel Synnaeve, Nicolas Usunier, Alexander Kirillov, and Sergey Zagoruyko. End-to-end object detection with transformers. In *European Conference on Computer Vision*, pp. 213–229. Springer, 2020.

Rewon Child, Scott Gray, Alec Radford, and Ilya Sutskever. Generating long sequences with sparse transformers. *arXiv preprint arXiv:1904.10509*, 2019.

Krzysztof Choromanski, Valerii Likhosherstov, David Dohan, Xingyou Song, Andreea Gane, Tamas Sarlos, Peter Hawkins, Jared Davis, Afroz Mohiuddin, Lukasz Kaiser, et al. Rethinking attention with performers. *arXiv preprint arXiv:2009.14794*, 2020.

Gonçalo M Correia, Vlad Niculae, and André FT Martins. Adaptively sparse transformers. *arXiv preprint arXiv:1909.00015*, 2019.

Zihang Dai, Zhilin Yang, Yiming Yang, Jaime Carbonell, Quoc V Le, and Ruslan Salakhutdinov. Transformer-xl: Attentive language models beyond a fixed-length context. *arXiv preprint arXiv:1901.02860*, 2019.

Giannis Daras, Nikita Kitaev, Augustus Odena, and Alexandros G Dimakis. Smyrf: Efficient attention using asymmetric clustering. *arXiv preprint arXiv:2010.05315*, 2020.

Jacob Devlin, Ming-Wei Chang, Kenton Lee, and Kristina Toutanova. Bert: Pre-training of deep bidirectional transformers for language understanding. *arXiv preprint arXiv:1810.04805*, 2018.

[5] https://github.com/kimiyoung/transformer-xl
[6] https://www.tensorflow.org/datasets/catalog/glue
[7] https://github.com/google-research/long-range-arena
[8] https://github.com/zhouhaoyi/Informer2020
[9] https://huggingface.co/roberta-base

Alexey Dosovitskiy, Lucas Beyer, Alexander Kolesnikov, Dirk Weissenborn, Xiaohua Zhai, Thomas Unterthiner, Mostafa Dehghani, Matthias Minderer, Georg Heigold, Sylvain Gelly, et al. An image is worth 16x16 words: Transformers for image recognition at scale. *arXiv preprint arXiv:2010.11929*, 2020.

Jonathan Heek, Anselm Levskaya, Avital Oliver, Marvin Ritter, Bertrand Rondepierre, Andreas Steiner, and Marc van Zee. Flax: A neural network library and ecosystem for jax. *Version 0.3*, 3, 2020.

Angelos Katharopoulos, Apoorv Vyas, Nikolaos Pappas, and François Fleuret. Transformers are rnns: Fast autoregressive transformers with linear attention. In *International Conference on Machine Learning*, pp. 5156–5165. PMLR, 2020.

Nikita Kitaev, Łukasz Kaiser, and Anselm Levskaya. Reformer: The efficient transformer. *arXiv preprint arXiv:2001.04451*, 2020.

Alex Krizhevsky, Geoffrey Hinton, et al. Learning multiple layers of features from tiny images. 2009.

Peter J Liu, Mohammad Saleh, Etienne Pot, Ben Goodrich, Ryan Sepassi, Lukasz Kaiser, and Noam Shazeer. Generating wikipedia by summarizing long sequences. *arXiv preprint arXiv:1801.10198*, 2018.

Yinhan Liu, Myle Ott, Naman Goyal, Jingfei Du, Mandar Joshi, Danqi Chen, Omer Levy, Mike Lewis, Luke Zettlemoyer, and Veselin Stoyanov. Roberta: A robustly optimized bert pretraining approach. *arXiv preprint arXiv:1907.11692*, 2019.

Ilya Loshchilov and Frank Hutter. Sgdr: Stochastic gradient descent with warm restarts. *arXiv preprint arXiv:1608.03983*, 2016.

Ilya Loshchilov and Frank Hutter. Decoupled weight decay regularization. *arXiv preprint arXiv:1711.05101*, 2017.

Andrew Maas, Raymond E Daly, Peter T Pham, Dan Huang, Andrew Y Ng, and Christopher Potts. Learning word vectors for sentiment analysis. In *Proceedings of the 49th annual meeting of the association for computational linguistics: Human language technologies*, pp. 142–150, 2011.

Chaitanya Malaviya, Pedro Ferreira, and André FT Martins. Sparse and constrained attention for neural machine translation. *arXiv preprint arXiv:1805.08241*, 2018.

Stephen Merity, Caiming Xiong, James Bradbury, and Richard Socher. Pointer sentinel mixture models. *arXiv preprint arXiv:1609.07843*, 2016.

Paul Michel, Xian Li, Graham Neubig, and Juan Miguel Pino. On evaluation of adversarial perturbations for sequence-to-sequence models. *arXiv preprint arXiv:1903.06620*, 2019.

Nikita Nangia and Samuel R Bowman. Listops: A diagnostic dataset for latent tree learning. *arXiv preprint arXiv:1804.06028*, 2018.

Hao Peng, Nikolaos Pappas, Dani Yogatama, Roy Schwartz, Noah A Smith, and Lingpeng Kong. Random feature attention. *arXiv preprint arXiv:2103.02143*, 2021.

Dragomir R Radev, Pradeep Muthukrishnan, Vahed Qazvinian, and Amjad Abu-Jbara. The acl anthology network corpus. *Language Resources and Evaluation*, 47(4):919–944, 2013.

Jack W Rae, Anna Potapenko, Siddhant M Jayakumar, and Timothy P Lillicrap. Compressive transformers for long-range sequence modelling. *arXiv preprint arXiv:1911.05507*, 2019.

Ali Rahimi, Benjamin Recht, et al. Random features for large-scale kernel machines. In *NIPS*, volume 3, pp. 5. Citeseer, 2007.

Aurko Roy, Mohammad Saffar, Ashish Vaswani, and David Grangier. Efficient content-based sparse attention with routing transformers. *Transactions of the Association for Computational Linguistics*, 9:53–68, 2021.

Sainbayar Sukhbaatar, Edouard Grave, Piotr Bojanowski, and Armand Joulin. Adaptive attention span in transformers. *arXiv preprint arXiv:1905.07799*, 2019.

Yi Tay, Dara Bahri, Donald Metzler, Da-Cheng Juan, Zhe Zhao, and Che Zheng. Synthesizer: Rethinking self-attention in transformer models. *arXiv preprint arXiv:2005.00743*, 2020a.

Yi Tay, Dara Bahri, Liu Yang, Donald Metzler, and Da-Cheng Juan. Sparse sinkhorn attention. In *International Conference on Machine Learning*, pp. 9438–9447. PMLR, 2020b.

Yi Tay, Mostafa Dehghani, Samira Abnar, Yikang Shen, Dara Bahri, Philip Pham, Jinfeng Rao, Liu Yang, Sebastian Ruder, and Donald Metzler. Long range arena: A benchmark for efficient transformers. *arXiv preprint arXiv:2011.04006*, 2020c.

Ashish Vaswani, Noam Shazeer, Niki Parmar, Jakob Uszkoreit, Llion Jones, Aidan N Gomez, Lukasz Kaiser, and Illia Polosukhin. Attention is all you need. *arXiv preprint arXiv:1706.03762*, 2017.

Apoorv Vyas, Angelos Katharopoulos, and François Fleuret. Fast transformers with clustered attention. *Advances in Neural Information Processing Systems*, 33, 2020.

Alex Wang, Amanpreet Singh, Julian Michael, Felix Hill, Omer Levy, and Samuel R Bowman. Glue: A multi-task benchmark and analysis platform for natural language understanding. *arXiv preprint arXiv:1804.07461*, 2018.

Jingdong Wang, Ting Zhang, Nicu Sebe, Heng Tao Shen, et al. A survey on learning to hash. *IEEE transactions on pattern analysis and machine intelligence*, 40(4):769–790, 2017.

Shuohang Wang, Luowei Zhou, Zhe Gan, Yen-Chun Chen, Yuwei Fang, Siqi Sun, Yu Cheng, and Jingjing Liu. Cluster-former: Clustering-based sparse transformer for long-range dependency encoding. *arXiv preprint arXiv:2009.06097*, 2020a.

Sinong Wang, Belinda Li, Madian Khabsa, Han Fang, and Hao Ma. Linformer: Self-attention with linear complexity. *arXiv preprint arXiv:2006.04768*, 2020b.

Thomas Wolf, Julien Chaumond, Lysandre Debut, Victor Sanh, Clement Delangue, Anthony Moi, Pierric Cistac, Morgan Funtowicz, Joe Davison, Sam Shleifer, et al. Transformers: State-of-the-art natural language processing. In *Proceedings of the 2020 Conference on Empirical Methods in Natural Language Processing: System Demonstrations*, pp. 38–45, 2020.

Haixu Wu, Jiehui Xu, Jianmin Wang, and Mingsheng Long. Autoformer: Decomposition transformers with auto-correlation for long-term series forecasting. *arXiv preprint arXiv:2106.13008*, 2021.

Yunyang Xiong, Zhanpeng Zeng, Rudrasis Chakraborty, Mingxing Tan, Glenn Fung, Yin Li, and Vikas Singh. Nystr\" omformer: A nystr\" om-based algorithm for approximating self-attention. *arXiv preprint arXiv:2102.03902*, 2021.

Zhilin Yang, Zihang Dai, Yiming Yang, Jaime Carbonell, Ruslan Salakhutdinov, and Quoc V Le. Xlnet: Generalized autoregressive pretraining for language understanding. *arXiv preprint arXiv:1906.08237*, 2019.

Andy B Yoo, Morris A Jette, and Mark Grondona. Slurm: Simple linux utility for resource management. In *Workshop on job scheduling strategies for parallel processing*, pp. 44–60. Springer, 2003.

Manzil Zaheer, Guru Guruganesh, Avinava Dubey, Joshua Ainslie, Chris Alberti, Santiago Ontanon, Philip Pham, Anirudh Ravula, Qifan Wang, Li Yang, et al. Big bird: Transformers for longer sequences. *arXiv preprint arXiv:2007.14062*, 2020.

Hang Zhang, Yeyun Gong, Yelong Shen, Weisheng Li, Jiancheng Lv, Nan Duan, and Weizhu Chen. Poolingformer: Long document modeling with pooling attention. *arXiv preprint arXiv:2105.04371*, 2021.

Haoyi Zhou, Shanghang Zhang, Jieqi Peng, Shuai Zhang, Jianxin Li, Hui Xiong, and Wancai Zhang. Informer: Beyond efficient transformer for long sequence time-series forecasting. *arXiv preprint arXiv:2012.07436*, 2020.

A EXPERIMENTAL SETTINGS

A.1 RE-EXAMINATION OF CONTENT-BASED SPARSE ATTENTION

For analysis, we pre-trained a 16-layer and 10-head Transformer on the WikiText-103 language modeling benchmark (Merity et al., 2016). A per-layer sinusoidal absolute positional encoding (Vaswani et al., 2017) is injected to the queries and keys before self-attention.

For Figure 1, we analyzed the queries and keys for the first 1024 tokens in the WikiText-103 validation data, and set the number of LSH buckets $B = 4$. We apply LSH to all the 10 attention heads in the 3rd Transformer layer. For Figure 2, we follow the same experimental setting.

A.2 LEARNING-TO-HASH

During the training stage, our final optimization objective $\mathcal{L}$ is a weighted combination of the task-specific objective L_{task} (e.g., cross-entropy loss in language modeling) and learning-to-hash objectives for all keys and queries, i.e., $\{\mathcal{L}_{Q_i}\}$ and $\{\mathcal{L}_{K_j}\}$ (See equation 13).

$$\mathcal{L} = \mathcal{L}_{task} + \frac{\lambda}{N \cdot L \cdot H} \sum_{i=1}^{N} \sum_{h=1}^{L} \sum_{h=1}^{H} (\mathcal{L}_{Q_i}^{L,H} + \mathcal{L}_{K_j}^{L,H}) \tag{19}$$

where λ, N, L, H denote the loss coefficient, the sequence length, the number of attention layers, and the number of attention heads per layer, respectively. Empirically, we set $\Lambda = 0.05$ and found it work well across different tasks.

A.3 LANGUAGE MODELING

We use the `base` setting of Transformer-XL (Dai et al., 2019) in our experiments, which consists of 16 Transformer layers. For each layer, the hidden size is set to 410, and the number of attention heads is set to 10. The dimension of feed-forward layer is set to 2100. All codes are implemented based on Flax (Heek et al., 2020) in JAX (Bradbury et al., 2018). The dropout ratio is set to 0.2. The batch size is set to 32. We use AdamW (Loshchilov & Hutter, 2017) as the optimizer, and set (β_1, β_2) to (0.9, 0.999). The peak learning rate is set to 3.5e-4. The model is trained for 20k steps with a 2k-step warm-up stage with a cosine learning rate decay (Loshchilov & Hutter, 2016).

A.4 NATURAL LANGUAGE UNDERSTANDING

We use the `base` setting of RoBERTa (Liu et al., 2019) in our experiments, which consists of 12 Transformer layers. For each layer, the hidden size is set to 768, and the number of attention heads is set to 12. The dimension of feed-forward layer is set to 3072. The RoBERTa pre-trained checkpoint is taken from the Transformers (Wolf et al., 2020) library. We use AdamW (Loshchilov & Hutter, 2017) as the optimizer, and set (β_1, β_2) to (0.9, 0.98). To fine-tune the pre-trained models, we search the optimization hyper-parameters in a search space including different batch sizes (16/32/48), learning rates ((1-5) * 1e-5), and the number of epochs (3-5). A 10% warm-up schedule and linear learning rate decay (Devlin et al., 2018) is applied.

A.5 LONG-RANGE-ARENA BENCHMARK

We follow the apples-to apples setting[10] of LRA benchmark and compare our method against other efficient attention variants. Specifically, we use a 4-layer Transformer with 256 hidden size and 1024 feed-forward layer size for the IMDb text classification task(Maas et al., 2011), a 4-layer Transformer with 256 hidden size and 1024 feed-forward layer size for the ListOps task(Radev et al., 2013), a 4-layer Transformer with 128 hidden size and 512 feed-forward layer size for the document retrieval task(Nangia & Bowman, 2018), and a 4-layer Transformer with 128 hidden size and 64 feed-forward layer size for the CIFAR10 image classification task(Krizhevsky et al., 2009). The models are trained for 20k steps with a 2k-step warm-up stage with a cosine learning rate decay (Loshchilov & Hutter, 2016).

[10] `www.github.com/google-research/long-range-arena#apples-to-apples-setting`

Table 4: Univariate long sequence time series forecasting results on two datasets (lower is better). †denotes that the results are taken from (Zhou et al., 2020).

Models		Ours - LHA		Informer†		LogTrans†		Reformer†		DeepAR†		Prophet†	
Metric		MSE	MAE	MSE	MAE	MSE	MAE	MSE	MAE	MSE	MAE	MSE	MAE
$ETTh_1$	24	**0.060**	**0.191**	0.098	0.247	0.103	0.259	0.222	0.389	0.107	0.280	0.115	0.275
	48	**0.088**	**0.236**	0.158	0.319	0.161	0.322	0.284	0.445	0.162	0.327	0.168	0.330
	168	**0.158**	**0.328**	0.183	0.346	0.187	0.355	1.522	1.191	0.239	0.422	1.224	0.763
	336	**0.219**	0.399	0.222	**0.387**	0.230	0.398	1.860	1.124	0.445	0.552	1.549	1.820
	720	**0.265**	0.437	0.269	**0.435**	0.273	0.463	2.112	1.436	0.658	0.707	2.735	3.253
$ETTm_1$	24	**0.016**	**0.102**	0.030	0.137	0.065	0.202	0.095	0.228	0.091	0.243	0.120	0.290
	48	**0.021**	**0.112**	0.069	0.203	0.078	0.220	0.249	0.390	0.219	0.362	0.133	0.305
	96	**0.054**	**0.180**	0.194	0.372	0.199	0.386	0.920	0.767	0.364	0.496	0.194	0.396
	288	**0.121**	**0.277**	0.401	0.554	0.411	0.572	1.108	1.245	0.948	0.795	0.452	0.574
	672	**0.403**	**0.572**	0.512	0.644	0.598	0.702	1.793	1.528	2.437	1.352	2.747	1.174

Table 5: Multivariate long sequence time series forecasting results on two datasets (lower is better). †denotes that the results are taken from (Zhou et al., 2020).

Models		Ours - LHA		Informer†		LogTrans†		Reformer†		LSTnet†	
Metric		MSE	MAE	MSE	MAE	MSE	MAE	MSE	MAE	MSE	MAE
$ETTh_1$	24	**0.475**	**0.469**	0.577	0.549	0.686	0.604	0.991	0.754	1.293	0.901
	48	**0.569**	**0.544**	0.685	0.625	0.766	0.757	1.313	0.906	1.456	0.960
	168	**0.883**	**0.706**	0.931	0.752	1.002	0.846	1.824	1.138	1.997	1.214
	336	**0.970**	**0.793**	1.128	0.873	1.362	0.952	2.117	1.280	2.655	1.369
	720	**1.021**	**0.805**	1.215	0.896	1.397	1.291	2.415	1.520	2.143	1.380
$ETTm_1$	24	**0.056**	**0.191**	0.323	0.369	0.419	0.412	0.724	0.607	1.968	1.170
	48	**0.088**	**0.236**	0.494	0.503	0.507	0.583	1.098	0.777	1.999	1.215
	96	**0.158**	**0.328**	0.678	0.614	0.768	0.792	1.433	0.945	2.762	1.542
	288	**0.219**	**0.399**	1.056	0.786	1.462	1.320	1.820	1.094	1.257	2.076
	672	**0.265**	**0.437**	1.192	0.926	1.669	1.461	2.187	1.232	1.917	2.941

A.6 Time Series Forecasting

We follow the experimental setup of Informer (Zhou et al., 2020). Specifically, the input length of recurrent component is chosen from $\{24, 48, 96, 168, 336, 720\}$ for the ETTh1, and chosen from $\{24, 48, 96, 192, 288, 672\}$ for the ETTm dataset. The layer of encoder is chosen from $\{6, 4, 3, 2\}$ and the layer of decoder is set as 2. The head number of multi-head attention is chosen from $\{8, 16\}$, and the dimension of multi-head attention's output is set as 512.

A.7 Computing Infrastructure

All the model training are conducted on a machine with 4 NVIDIA Ampere A100 40GB GPUs and 64 AMD EPYC 7713 64-Core Processor in a Slurm (Yoo et al., 2003) system. The evaluation of the inference throughput is performed on a stand-alone machine with 1 NVIDIA Tesla V100 32GB GPU.

B Additional Experiments on Time Series Forecasting

We also evaluate our model on time series forecasting tasks. We use the ETT (Electricity Transformer Temperature) dataset (Zhou et al., 2020), which contains 2-year data from two separated counties in China. $ETTh_1$ is a dataset for 1-hour-level, while $ETTm_1$ is a dataset for 15-minute-level. Each data point consists of the target value "oil temperature" and 6 power load features. The train/val/test is 12/4/4 months. The Mean Squared Error (MSE) metric and Mean Average Error (MAE) metric are used as the evaluation metrics. We use a LHA/local hybrid variant similar to variant (d) in Section 5.1.

In univariate forecasting setting, all the seven features are used as input and "oil temperature" is the prediction target. The univariate evaluation results can be found in Table 4. We can see that

LHA significantly improve the performance of state-of-the-art for most settings, while slightly underperforms Informer (Zhou et al., 2020) in two settings of ETTh_1 dataset. This verifies the effectiveness of LHA on time series data.

In multivariate forecasting setting, all the seven features are the prediction targets. The multivariate evaluation results can be found in Table 5. We can see that LHA significantly improve the performance of state-of-the-art for all settings, which further demonstrates the effectiveness of the proposed LHA method.

C PROOF

We follow the notations in (Daras et al., 2020). Let $\mathcal{C}^B$ the set of all possible assignments in B balanced non-overlapping clusters. A specific assignment is denoted by $\mathcal{C}_t^B$ and there are T possible such assignments:

$$\mathcal{C}^L = \{\mathcal{C}_1^B, C_2^B, ...\mathcal{C}_T^B\}. \tag{20}$$

$$\mathcal{C}_t^B = \{c_1, c_2, ..., c_B\} : \quad \begin{cases} c_i = \{Q_1^i, ..., Q_{\frac{N}{B}}^i, K_1^i, ..., K_{\frac{N}{B}}^i\} \quad c_i \subseteq \mathcal{Q} \cup \mathcal{K}, \ \ \forall i \in \{1, ..., L\} \\ c_x \cap c_y = \varnothing \quad \forall c_x, c_y \in \mathcal{C}_t^B \end{cases} \tag{21}$$

We have the following lemma, which is referred as the max-mass problem:

Lemma 1. *(Daras et al., 2020) The optimization problem:*

$$\max_{\mathcal{C}_t^B \in \mathcal{C}^B} \sum_{(Q_i, K_j) \in \mathcal{C}_t^B} Q_i \cdot K_j \tag{22}$$

is NP-hard.

The main idea of the proof is to show that solving polynomially the above problem would mean that we could also solve in polynomial time the 3-DM, which is known to be NP-complete. Please refer to (Daras et al., 2020) for the detailed constructive proofs. Next, we show how to use this lemma to prove Theorem 1.

Proof of Theorem 1. Let $\{Q_i\}$ and $\{K_j\}$ denote the query and key sets that we consider for computing the attention utility. We can first construct the new query set $\mathcal{Q}'$ and key set $\mathcal{K}'$ such that

$$Q_i' \cdot K_j' = \frac{e^{Q_i \cdot K_j}}{\sqrt{d_h}}, \quad \text{where} \quad Q_i' \in \mathcal{Q}', K_j' \in \mathcal{K}'$$

This can be achieved by applying SVD to the matrix of $\left(\frac{e^{Q_i \cdot K_j}}{\sqrt{d_h}}\right)_{ij}$. Next, we construct another query set $\mathcal{Q}''$, such that

$$Q_i'' = \frac{Q_i'}{\sum_{j=1}^n Q_i' \cdot K_j'}$$

The problem of finding the optimal attention utility, i.e.,

$$\arg\max_{\mathcal{C}_t \in \mathcal{C}} \text{AU}(\mathcal{C}_t) = \sum_{(Q_i, K_j) \in \mathcal{C}_t} A_{ij}$$

is thus equivalent to the problem in Lemma 1, with $\mathcal{Q}''$ and $\mathcal{K}'$ as the query and key sets, which is proven to be NP-hard. □

D ALGORITHM

We present a detailed pseudo-code implementation for LHA in Algorithm 1.

Algorithm 1 Single-layer Single-head Learning-to-Hash Attention (LHA)

Queries, Keys and Values: $Q, K, V \in \mathbb{R}^{N \times d_h}$
Query/Key Hash Functions:
Attention Utility Loss Weight: λ
if causal mask **then**
    $Q_{score} \leftarrow \mathrm{softmax}(H_Q(Q) + H_K(K))$ ▷ $B \times N \times d_h$
    $K_{score} \leftarrow Q_{score}$
else
    $Q_{score} \leftarrow \mathrm{softmax}(H_Q(Q))$ ▷ $B \times N \times d_h$
    $K_{score} \leftarrow \mathrm{softmax}(H_K(K))$ ▷ $B \times N \times d_h$
$W \leftarrow N/B$ ▷ bucket size
$Q_{idx} \leftarrow \text{top-}\{\sqrt{2}\mathrm{W}\}(Q_{score})$ ▷ $B \times N \log(N)$
$K_{idx} \leftarrow \text{top-}\{\sqrt{2}\mathrm{W}\}(K_{score})$ ▷ $B \times N \log(N)$
$Q' \leftarrow \mathrm{gather}(Q, Q_{idx})$ ▷ $B \times W \times d_h$
$K' \leftarrow \mathrm{gather}(K, K_{idx})$ ▷ $B \times W \times d_h$
$V' \leftarrow \mathrm{gather}(V, K_{idx})$ ▷ $B \times W \times d_h$
$A \leftarrow Q'(K')^T$ ▷ $B \times W \times W \times d_h$
if causal mask **then**
    $A \leftarrow \mathrm{mask}(A)$ ▷ $B \times W \times W$
$A \leftarrow \mathrm{softmax}(A).$ ▷ $B \times W \times W$
$V' \leftarrow A \cdot V'$ ▷ $B \times W \times W \times d_h$
$X \leftarrow \mathrm{scatter}(K_{idx}, V')$ ▷ $B \times W \times d_h$
$\boldsymbol{\psi} = \mathrm{AU}_Q(Q, K)$ ▷ $B \times N$, Equation 16
$\boldsymbol{\psi'} = \mathrm{AU}_K(Q, K)$ ▷ $B \times N$, Equation 17
$\mathcal{L}_{AU} = \lambda \cdot KL(\boldsymbol{\psi} \| Q_{score}) + \lambda \cdot KL(\boldsymbol{\psi'} \| K_{score})$
return $X, \mathcal{L}_{AU}$

E VISUALIZATION

We visualize the full attention map of an attention head in a Transformer model pre-trained on WikiText-103 dataset in Figure 4, and visualize its LHA counterpart and LSH counterpart in Figure 5 and Figure 6, respectively. We do not apply the causal mask when calculating the attention weights. The attention utility of LHA and LSHare 0.461 and 0.335, respectively. From the visualization, we can see that LHA is able to better approximate the full attention with learnable hash functions.

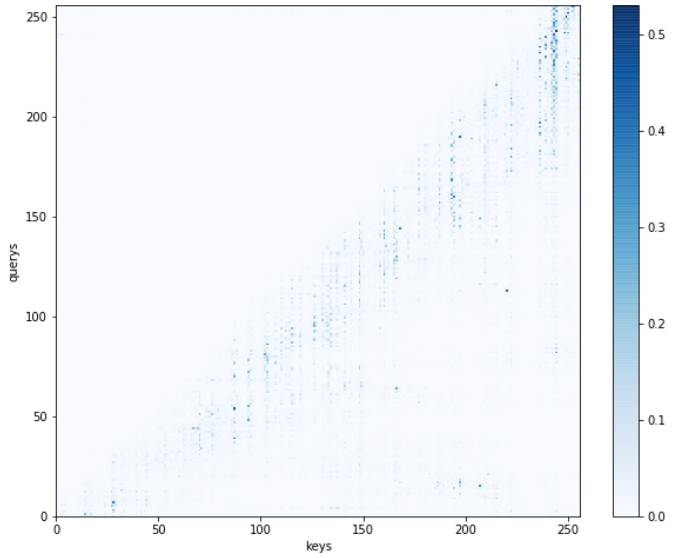

Figure 4: Attention map of full attention.

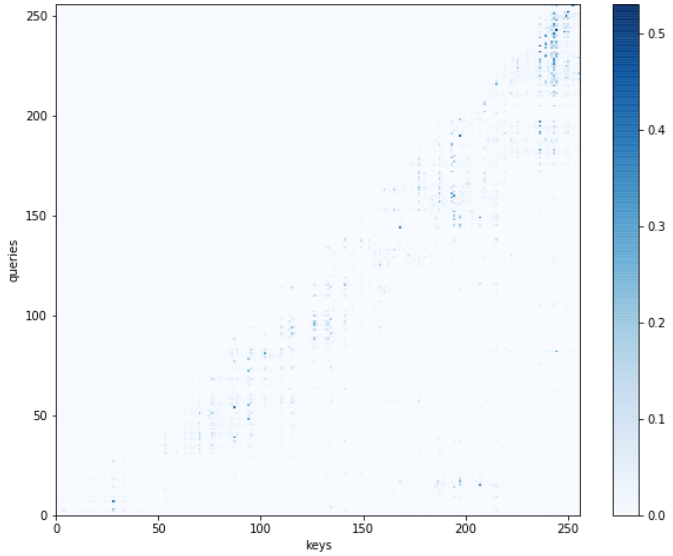

Figure 5: Attention map of Learning-to-Hash Attention (LHA) with 0.461 attention utility.

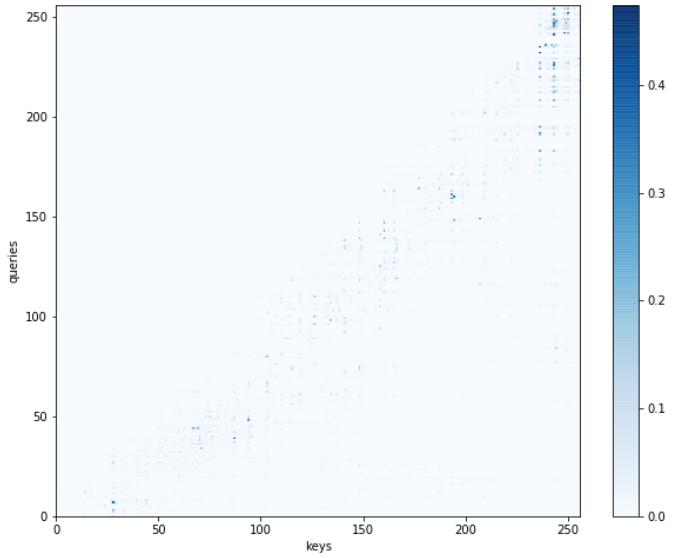

Figure 6: Attention map of LSH attention with 0.335 attention utility.